

OPTIMIZATION AND REDESIGN OF AN ELECTRON SPECTROMETER FOR HIGH RESOLUTION GAS PHASE UV PHOTOELECTRON, AUGER ELECTRON AND ION FRAGMENT SPECTROSCOPY

by

Peter Baltzer, Björn Wannberg and Mats Carlsson Göthe.

Uppsala University, Institute of Physics,
Box 530, S-75121 Uppsala
Sweden

Abstract.

Extensive modifications of an electrostatic electron spectrometer of the hemispherical type are described. The purpose of the modifications is to make the instrument more suitable for high resolution gas phase spectroscopy. The changes concern substitution of electrical adjustments for mechanical precision, improved flexibility in focusing and a new system of computer controlled power supplies and detector interface. The instrument is also used for energy analysis of positive ions. Conversion between positive and negative particle analysis is achieved simply by reversing the polarities of all relevant voltages by a number of switches. A gas cell with internal heating is described. The influence of gas cell conditions on resolution is shortly discussed. The computer programs used for spectrometer control, data acquisition, spectrometer optimization and calibration are described.

1. INTRODUCTION.

Electron spectroscopy is used generally to investigate the electronic structure of atoms, molecules and condensed matter. A great variety of instrumental designs have been reported and applied in different fields of research ^{1,2}. Different types of investigations usually require optimization of different properties of the instruments. Hence, the optimization of an instrument for a certain type of investigation often leads to design solutions which are incompatible with the requirements for optimization with respect to other types of studies. It is therefore difficult, if not impossible, to design multipurpose spectrometers, which are capable of providing results of high quality in all fields of application. A clear border-line can be drawn between research performed in the high vacuum ($\approx 10^{-6}$ torr range) and the ultra-high vacuum range ($\leq 10^{-9}$ torr). The latter is necessary in order to study surfaces and adsorbates on surfaces. In general, pressures in the order of 10^{-11} torr are required for obtaining high quality data in surface science. Such extremely low pressures require in the first place a stainless steel design and facilities for baking. These requirements lead to a comparatively strained construction with metal seals at all flanges. Dismounting and reassembling can therefore be quite time-consuming. In surface science where the sample gas load is exceedingly small this does not pose too great problems. Furthermore, the photoelectron lines from solid surfaces tend to be much broader than what can be obtained in the gas phase, so the demands on high resolution conditions are not as pronounced as in gas phase studies. In high resolution gas phase studies where the quality of spectra depends on clean surfaces with well-defined potentials in the interior of the spectrometer, not withstanding continuous exposure to comparatively high gas pressures, it is necessary to dismount the instrument regularly for re-conditioning. Of vital importance for successful research is then that the re-conditioning and mounting is a simple routine procedure.

Other borderlines can be identified between photoelectron spectroscopies using resonance UV-, X-ray or synchrotron radiation for excitation of spectra. These may perhaps to a larger extent be connected to the difficulties for a single research group to work in several different fields or energy regions than to difficulties of obtaining instrument designs which are suitable for different types of excitation sources. However, even in these cases it is easy to identify different requirements on the instruments. If one wants to work with the highest possible resolution in gas phase studies it is necessary to consider the factors which determine the photoelectron line widths. In the case of UV-excitation the line widths in ordinary instruments, employing a gas cell to define the ionization volume, can be better than 10 meV (FWHM). The line width is primarily due to rotational and Doppler broadenings as well as changes in work function due to deposition of sample gas on the gas cell, lens and aperture slits, and finally plasma potentials in the gas cell. The plasma potential develops instantaneously (order of nanoseconds) in the gas cell. Therefore line shifts and line broadening caused by this potential will follow any intensity variations in the excitation source. Changes in work function can be so fast, particularly for reactive gases, that this factor determines the resolution shortly after the introduction of the target gas in the ionization volume. On the other hand, the resolution in monochromatized X-ray excited spectra attained in instruments built with special regard to high resolution recordings is primarily set by the width of the X-rays, which is of the order of 0.2 eV at

best. At this resolution level, all the above mentioned effects usually give very small contributions provided that the spectrometer surfaces are properly treated from the outset. The importance of easy access to the interior of the spectrometer is thus usually much more pronounced in the UV-excitation case than for X-ray excitation. From this point of view different design principles may provide optimal conditions for studies by these different excitation sources. Similar considerations can be made for various aspects of the research and usually each of them requires in some way a unique design for optimization of the results. It is therefore perhaps not surprising that a great variety of spectrometer designs have been reported in the literature. A recent review of instruments for photoelectron spectroscopy has been given by Leckey², who also discusses such subjects as multidetection techniques.

In the present report we describe the redesign of a spectrometer which was originally built for UV- and electron impact excitation for studies of both gaseous samples and for surface physics. The original design has been previously described ², and in the present paper we focus on the points where changes have been made. The research groups in Uppsala using electron spectroscopy have to some extent specialized on different fields of research and in the first place the UHV-compatibility of the present instrument could be abandoned since the surface physics is performed on another instrument. The instrument has therefore been optimized for gas phase work at high resolution. Both the UV- and electron impact excitation facilities have been retained and the UV-source can also be equipped with a polarizer for angle resolved studies of photoelectron spectra. The old design used a gas cell to define the ionization volume and in the present work this basic type of construction has been retained. However, the detailed shape of the gas cell has been varied in order to study work function changes and plasma potentials in the ionization volume. The results of these studies are reported briefly in a separate section below. Application of a supersonic-jet arrangement to the spectrometer in order to reduce the influences from Doppler- and rotational broadenings is highly desirable and will constitute a part of the continuous development of the experimental equipment.

In general, high resolution measurements in UV-excitation mode requires careful alignment of focussing elements. However, this does not necessarily mean that all demands must be fulfilled by perfect alignment of the mechanical components. It may instead be a better solution to relax the demands on these elements somewhat and use compensating electric fields for the final adjustment to control the path of the electrons through the electron lens and final aperture prior to the kinetic energy analysis. Electrostatic focussing has been used since long in order to obtain an image of the sample on the entrance slit of the energy analyzer and has been found to work excellently. The mechanical precision on electric focussing elements and apertures of such devices need not be extremely high. Furthermore, and perhaps even more important, the electric fields are easily varied from voltage supplies outside the spectrometer and no provisions are necessary for adjusting mechanical components inside vacuum after the spectrometer has been assembled. As was pointed out above, mechanical simplicity is favourable when the high resolution aspect is stressed. The difficulties involved in producing and maintaining electrode potentials which are homogeneous to better than ± 0.1 V have been known for a long time⁴. In order to maintain high resolution under dirty-gas load conditions, repeated cleaning and coating with colloidal graphite is essential. The parts to coat are, in descending order of importance, the gas cell, the entrance slit preceding the analyzer, the

analyzer and the lens electrodes. The present paper gives a detailed description of the mechanical design as well as the elements used to control the electron path and the voltage control units.

The voltage supplies and connections to the spectrometer have been designed specifically for the use in high resolution spectroscopy, i.e. high stability, low noise and induced voltages but no current load. With the application to spectroscopy of positive ions in mind the electrical connections were designed in order to make it easy to change the polarities of the relevant voltages. The power supplies and coupling schemes are described below.

Photon impact is used for photoelectron spectroscopic investigations at high resolution. In test recordings on the new spectrometer system line widths of the order of 5 meV (FWHM) have been obtained for the rare gases (cf. Fig. 1). The first application concerned the vibrational structure of HCl and DCl where in particular the barrier against predissociation in the $A^2\Sigma^+$ state has been determined by the observation of vibrational levels disappearing at a certain energy ⁵.

Electron impact excitation is used primarily for Auger electron spectroscopy and for ion fragment spectroscopy. In both cases the high resolution property of the instrument is useful because it permits the studies to be performed at a resolution level where the line width practically exclusively depends on the life-time of the states involved in the Auger case and on Doppler broadening in the ion case. Recent studies have included isotope effects on the vibrational structure of spectra from HCl and DCl ^{6,7} as well as from HBr and DBr ⁸. In these spectra the line-width of the order of 100 meV is determined by the singly ionized core-hole state which forms the initial state of the Auger transition. Since the vibrational spacings are larger than this value the structure could be well resolved. Other recent studies have been performed on the Auger electron spectrum of NO₂ ⁹ and H₂S ¹⁰. In the spectrum of the latter well resolved vibrational structure has been observed. It can be noted that optimization of the resolution is difficult to perform directly from the Auger lines due to high background and large linewidths. Therefore, we use the UV-source in order to optimize the conditions for each sample gas from the narrow photoelectron lines.

With electron impact ionization, many molecules dissociate, leaving at least one positively charged fragment, the energy of which can be measured. In the case of diatomic molecules only two fragments can be formed so at most two overlapping spectra are observed. In particular, if one of the elements is very light compared to the other one, essentially one ion spectrum corresponding to that element is obtained. Such studies have been performed for the first time on the abovementioned molecules HCl/DCl, HBr/DBr, and HI. The proton and deuteron spectra of these molecules show a line structure which can be associated primarily with final states in the doubly ionized systems generated both by Auger and direct two-electron excitation processes ¹¹. In these spectra proton energies as high as 25 eV have been observed, corresponding to dissociation from repulsive electronic states. However, high energies are also obtained from predissociative states with tunneling barriers. In recent studies also photon induced dissociation has been observed for N₂, H₂S ¹⁰ and HI ¹². Using radiation from VUV line sources (He or Ne) almost exclusively dissociation from singly ionized states is observed. As in the case of Auger spectroscopy, optimization of the focussing conditions has to be performed using the narrow photoelectron lines. In this case, one cannot expect conditions to be identical,

however, since work function modifications of the internal field structure has a definite polarity.

2. EXPERIMENTAL DETAILS.

2.1. Reconstruction aims.

With regard to the arguments presented above the redesign of the instrument was made with particular attention to the following requirements:

1. Dismounting and mounting of the entire instrument should be possible with minimum effort.
2. Need for mechanical perfection should, wherever possible, be minimized by providing means for electric or very simple mechanical run-time adjustments.
3. The number of independent electrodes should be minimal in order to simplify the optimization.
4. The vacuum requirements should be relaxed to the microtorr level, thereby permitting the use of elastomer seals and 2-4 bolts per flange. (On contrast, the analyzer compartment was earlier sealed with an aluminum-foil gasket and tightened with 50 bolts, which made access to the interior very laborious.)
5. The lens should be easy to remove and replace, without realignment of its slits being necessary.
6. The gas cell should be moveable in all three directions and rotatable around the longitudinal axis of the lens during operation to permit optimization of target position, and it should be removable for recoating, without loss of alignment.

2.2. The analyzer.

The basic shape of the analyzer is a truncated hemisphere, using only a zone of ± 22.5 degrees around the equatorial plane. The central radius is 144 mm, while the radii of the two electrodes are 113.6 and 174.4 mm, respectively. In the original design, the field was terminated on all edges by a system of 16 electrodes, each of which was connected to the voltage corresponding to its particular radius via a voltage divider. The voltage divider was designed to give the ideal spherical shape of the field, but work function deviations could not be corrected. Although the voltages of the individual electrodes could in principle be adjusted, any experimental optimization of this large number of variables is of course impracticable. The use of terminating electrodes simulating a spherical field on the exit plane, up to the edges of the detector multichannel plane, which itself is an equipotential surface, also led to undesirable shapes of the field at the edges of the detector.

The imaging properties of a general toroidal field depend up to second order only of the ratio between the two radii of curvature of the equipotential surface at the central trajectory and of the derivative of this ratio with respect to the main radius¹³. As long as the second order description of the analyzer properties is valid, there are thus just two degrees of freedom, and any system of electrodes giving the same values for these two quantities

should be equivalent. In a spectrometer where an input lens system limits the entrance solid angle, this is a good approximation. Consequently, the elaborate system of terminating electrodes was replaced by two strips, close to the inner and outer edges of the gaps between the two main electrodes. These strips are mounted on the original base plate for the terminating electrodes, and in the gap between them the base plate, which is connected directly to the retardation voltage, completes the fringing field. A cross section of the analyzer with the new fringing field electrodes is shown in Fig. 2. Apart from the simplification this means with respect to disassembly for cleaning, it also makes empirical adjustment of the field shape for best resolution feasible, since there is in principle no reason to assume that the perfect spherical field should be optimal under all circumstances. For example, a straight entrance slit which is simple to manufacture, will produce a slightly curved line at the detector if the analyzer field is spherical. However, by adjusting the two voltages of the terminating electrodes a straight line can be obtained, leading to improved resolution since the multidetection system assumes straight lines.

This arrangement of fringing field electrodes is also applied on the entrance plane. On the exit plane, the base plate is left naked and on the same potential as the front of the detector. The optical properties of the exit fringing field for this geometry are well-known¹⁴. The main effect is a second order change of the energy dispersion, which just compensates for the second order dependence of the dispersion on energy in the main hemispherical field. Thus, the energy scale on the detector is more nearly linear with this electrode geometry.

The focusing properties of the analyzer depend not only of the shape of the field, but also of the entrance angle of the electron beam, and the optimum shape of the field is strongly dependent on this angle. For a perfect hemispherical field, it is easy to show that the main effect of a small radial angle between the central trajectory and the tangent to the sphere at the entrance point is a shift in the position of the radial image plane. Since the aperture error of the hemispherical field is $\Delta r = -2r_0\alpha^2$, the radial defocusing for a centre beam angle α_0 and an angular spread α is $-4r_0\alpha\alpha_0$ in the nominal image plane, and consequently, the actual radial image plane is displaced through the angle $4\alpha_0$. The axial imaging is to first order not changed by a change in the radial entrance angle. The change in image plane position is shown schematically in Fig.3.

In order to adjust the entrance direction of the electrons into the analyzer, a pair of deflection electrodes are placed immediately after the exit slit of the lens i.e. the entrance slit of the analyzer. These electrodes consist of straight cylindrical rods with a diameter of 2 mm and a separation of 20 mm. The primary purpose of these deflection electrodes was to be able to compensate for errors in entrance direction caused by inaccuracies in the lens alignment, by residual magnetic fields or by work function effects. They also provide, however, one extra degree of freedom in the adjustment of the electron optics for optimum resolution. It is found empirically that there is a very strong interdependence between these deflection voltages and the corresponding optimum setting of the fringing field electrodes. Already quite small deflections of the beam result in optimum values of the fringing field voltages which deviate significantly from those giving the best spherical field. One example of this is given in Fig. 4, which shows the width of a photoelectron line (averaged over the width of the detector) as a function of the two fringing field voltages. The deflection voltage was here set to give approximately optimum conditions.

Originally, the analyzer electrodes were separated by 18 individually selected mica plates of slightly different thickness. To simplify the construction of the analyzer and also get rid of problems with short-circuits when coating the interior with colloidal graphite, the mica-plates were replaced by two teflon-bands. Graphite-suspension does not spread on teflon as easily as on mica, when accidentally put on. By performing computer calculations of the electric potential in the analyzer we found that the reduction in precision from this type of spacer gives negligible contribution to the resolution.

2.3. The accelerating/retarding lens.

A number of modifications have been introduced in the lens system, both for reasons of simplified mounting/cleaning operations and for electron optical reasons. A schematic layout of the lens system is given in Fig. 5. Since in VUV-excited photoelectron spectra one rarely has reason to trade off resolution for intensity, and one in such cases anyhow has the option to choose a higher analyzer pass energy, the mechanically complicated system of interchangeable slits was abandoned, and fixed aperture and object slits, manufactured from thin copper foils, were introduced. The aperture slit was removed from its earlier position in the gap between the last two lens elements and placed in the field-free region inside the long lens element. The rationale for this was primarily to eliminate the possibility of an unwanted lens action of this slit, should its potential deviate from that corresponding to its position. Neither the new nor the old position of the aperture slit is ideal from the electron-optical point of view, since the entrance solid angle it defines in the analyzer is in both cases dependent on the retardation or acceleration ratio. An obvious further modification would be to place both slits after the last active lens gap, with a relative distance of 20 - 30 mm, where the object slit is the last one.

Correction of the beam direction inside the lens in order to obtain maximum intensity was earlier done with a pair of current coils, creating a small magnetic deflection field. These coils have been replaced with a semi-cylindrical electrostatic deflection electrode immediately after the aperture slit. The function of this deflection is to correct for misalignment of the exciting photon or electron beam with respect to the lens axis, and also to compensate for residual magnetic fields. With typical electron energies at the position of the deflector of a few hundreds of eV, the deflection voltages applied for best intensity are a few volts. This simple semicylindrical shape of the deflection electrode, together with a symmetrically placed dummy on lens potential gives a reasonably pure dipole field in the region of the beam.

One further simplification which has been introduced in the lens system is the permanent connection of the first focussing element to the retardation voltage. Although a small deviation of this element's potential from the retardation voltage would be necessary to keep the magnification of the lens system constant, experience has shown that intensities are hardly changed by this simplification. This means that the only remaining focussing voltage, which is applied to the long lens element, can be described by one universal curve, by representing the ratio of focussing voltage to the analyzer pass energy as a function of the ratio between the initial electron energy and the pass energy. This curve is shown in Fig. 6. The focusing voltage for any combination of initial and pass energy is

calculated by a cubic spline approximation to this curve, requiring only a small number of parameters for its definition.

The exit element of the lens has been modified in order to accommodate the revised slit arrangement and the deflection pins mentioned above.

2.4. The gas cell.

The gas cell, in which the ionization takes place, is formed simply from a cylindrical tube with a slit of 0.2mm x 4mm for the outgoing electrons and two holes for the incoming and outgoing photon flux (cf upper part of Fig. 7). The slit defines the first differential pumping stage where the pressure is reduced from about 10 mtorr in the gas cell. The final pressure in the analyzer at normal recording conditions is of the order of 10^{-5} torr.

Good surface conditions in the gas cell are a necessary provision for high resolution spectra. Such conditions are obtained by a fresh layer of colloidal graphite coating applied to all surfaces. The shape of the gas cell also influences the resolution. Since the ionization region is not an infinitely thin string in the gas cell, any potential gradient inside it may give rise to a line broadening. This was observed in an asymmetrically extended gas cell originally designed to minimize the influence of local differences in work function. In this geometry large line shifts of up to 0.5 eV were observed along with substantial line broadenings with increasing gas pressure, still within otherwise usable pressure range. This result was interpreted as an effect of an asymmetrical plasma potential developed across the radiation beam. The large line shifts show that even small variations in the beam intensity or gas pressure may cause variations in the line position which give rise to a non-negligible line broadening. This effect can be observed even with the normal gas cell, although to a much lower degree. Fig. 8 is an example of this, showing a diagram of the peak position versus the relative intensity of the photoelectron line. In order to investigate the origin of the shift further, tests were made with a potential compensating electrode inside the gas cell behind the ionization region (cf lower part of Fig. 7). A gradual change in linewidth with increasing electrode voltage was observed and the maximum resolution was obtained at approximately 1 volt at a pressure of about 200 mtorr in the gas cell.

To allow the study of substances with low vapour pressure at room temperature it is desirable that the gas cell can be heated to a given stable temperature. Such a device was constructed with the specifications that the temperature should be continuously variable between room temperature and 200C° and with a long term stability of $\pm 1\text{C}^\circ$.

In low energy electron spectroscopy the tolerable magnetic fields in the region where the electrons move are very small. To overcome the difficulty associated with magnetic fields from the heater current, it was decided to use high frequency current, strictly without DC-component, to energize the heater element. For the reason of simplicity, this was chosen to be a low voltage incandescent bulb of the halogen filled quartz type, rated 12V/20W. The quartz envelope also protects the tungsten filament from corrosion. The really important advantage with this solution is, that the magnetic field from the filament can be shielded by any conductor due to the induced eddy currents. In our case, using aluminum

for the gas cell and 20 kHz heater voltage, the characteristic damping depth is 0.4 mm. Moreover, the use of AC voltage leads to simple power regulation by using pulse width modulation (PWM) technique without rectifying losses.

In our application, the absolute value of the temperature is of secondary importance, since it is adjusted for each substance to give the proper gas cell pressure for a convenient spectrum count rate. This allowed the use of an uncalibrated NTC resistor in a glass bead as the sensing element. This is preferable to a thermocouple because of its higher voltage sensitivity. The controller for the oven is constructed as shown in Fig. 9. Note the output transformer that guarantees DC-free power. The construction is basically a PI-regulator, tailored to the gas cell thermal mass, feeding a PWM stage regulating between 0 to 50 % duty cycle. This 40 kHz rectangle wave is fed to a power MOS transistor driving the transformer primary. The DC supply voltage is 24 V requiring a transformer stepdown ratio of 4:1.

To show that the heating does not impair the instrument resolution, a spectrum of ammonium chloride at approx. 150C is shown in Fig. 10. The substance is clearly seen to decompose in HCl and NH₃

3. SPECTROMETER CONTROL AND DATA ACQUISITION.

3.1. General layout.

The spectrometer is controlled from an IBM PC/AT computer via an IEEE-488 parallel bus (Fig. 11). Since ground loop currents and voltage transients are known to give rise to serious problems concerning voltage stability and also may be destructive for electronic components, the system was designed to avoid any possible ground loops. The means to achieve this include:

1. Every voltage supply is fully floating up to the highest possible system voltage (6kV).
2. The data transmission cable between the main computer and the spectrometer has been optically isolated in both ends, partly since it could not be guaranteed that the spectrometer and computer are connected to the same mains grounding point, and partly to avoid the loop otherwise created.

As a consequence of point 2 above the IEEE bus could not be used generally in the system, since it is virtually impossible to isolate optically. The bus is therefore used solely as a fast standard interface to the spectrometer system in order to facilitate replacement of the main computer. For the communication with the spectrometer an optoisolated high speed serial link (500 kBaud) is used. The interface between the IEEE bus and the serial link is placed directly at the main computer. This interface has its own dedicated microprocessor (Motorola 68000) and can be considered as a part of the control and detection system. In addition to the conversion from IEEE to serial code, the computer has some time-saving tasks described below.

3.2. The detection system.

For detection of the charged particles a microchannel plate (MCP) detector is used. It contains two microchannel plates mounted in a chevron configuration which are followed by a phosphor screen which transforms the electron pulses into light pulses (cf Fig. 12). The screen is viewed by a commercially available CCD TV-camera (SONY XC-37) connected via a dedicated microcomputer to the operator's computer system described below. This computer is made from the same hardware as the Bus/Link computer, but with a different machine-language program. It performs a number of different operations:

1. Real-time acquisition of particle impact signals from the TV-camera.
2. Energy scale linearisation to compensate for the non-linear dispersion of the energy analyser using a correction table residing in an onboard RAM. This table can be readily updated from the main computer. This is crucial for high resolution work since the dispersion function does not lend itself to precise mathematical treatment and is sensitive to surface conditions.
3. Performs all data processing during swept recording of spectra (Fig. 12).
4. Displays active window and real-time energy spectrum on a TV-monitor, that also shows the flashes from the phosphor screen. The video signal to the monitor is optically isolated.

In front of the microchannel plates a high transmission mesh is placed, with an open area ratio of about 80%. This mesh is connected to the acceleration voltage (called AV in Fig. 11) on the base plate. By this arrangement the detector front voltage can be set to accelerate ions, without distorting the field in front of the detector, thus enhancing the detection efficiency for such particles. A good efficiency for proton detection requires about 100 eV kinetic energy while for electrons 10-20 eV is sufficient. At higher voltages the detector background tends to increase. In the case of electron detection, this is mainly due to secondary electrons from the outer analyser wall, but for positive ions the reason is probably an ion-feedback mechanism. The mesh is in this case positive with respect to the MCP front and ions created in a channel are reflected. A support for this interpretation is the fact that, in the ion-case, the background at elevated mesh-voltage consists mainly of "switched-on" channels i.e bright spots lasting for periods of the order of one second.

3.3. Voltage supplies.

The voltage supplies were developed to meet the following requirements:

1. Linearity over the range should be better than 10 ppm (always referred to the maximum attainable voltage of the supply).
2. Short-term drift (1 day) better than 10 ppm.
3. Maximum voltage of unit should be 100, 600, 1500 and 6000 volts.
4. Temperature stability better than 2 ppm/degree Celsius.
5. Ripple and noise at any spectrometer electrode less than 10 ppm.
6. Every supply should be floating up to 6000 volts and present as low capacitance as possible to ground to minimize induced hum and noise from looped connections.

7. The supply should be computer controlled with the full voltage range divisible in at least 4000 equal steps. This is demanded by the most critical lens and analyzer voltages but is not sufficient to allow scanning of the AV-voltage (cf Fig. 12), with the required accuracy. To meet this demand, this voltage is produced by using a high-precision DAC-module in series with the supply, using the latter merely as a highly stable platform for the DAC-module. This can be adjusted in 0.2 mV steps over a ± 13.1 volt range.

A schematic drawing of the voltage supply is shown in Fig. 14. The power feed to the supply is 12 Volt DC 300 mA. This is delivered to an on-board 20 kHz switching DC/DC-converter designed for low capacitance and low common-mode transients. It delivers ± 12 V regulated system voltage and raw 20 V to the HV-generator. This is a low-power flyback-type converter capable of delivering 6 kV 0.2 mA. It is controlled by pulse-width modulation to deliver approximately the desired voltage. This stage is followed by a fine-adjustment section consisting of the R and C in Fig. 13. The low-voltage end of C is connected to the output of a nullvoltmeter circuit and consequently allows instant correction of short-term variations (ripple and small adjustments of voltage settings) of the output voltage. Of course persistent deviations could not be corrected in this manner, but have to be fed to the HV-generator's control input.

The problem is hence reduced to that of accurately measuring the actual output voltage. It can be subdivided in Voltage division and Reference voltage. The reference is an on-chip temperature stabilized zener reference which has a temperature coefficient of $<1\text{ppm/C}$ but 5% tolerance on the zener voltage, which is about 6.2 V. To avoid drifts it was decided not to make any calibration on board, but instead allow every supply to have its own set of calibration constants which are stored in the main computer. The reason to choose this solution in favour of a precision-calibrated reference (and precision voltage divider) was that in the latter case stability would have to be traded off and costs had increased dramatically.

The stable zener voltage is then fed to an analog switch, whose output is toggled between the zener voltage and zero volt. The repetition frequency is optional, but is in our case set at 250 Hz. The duty cycle of this rectangle wave is controlled by the computer. Next to the switch is a low-pass filter, made of 3 RC-links. The time constant is selected to get less than 1 ppm 250-Hz-ripple, and the capacitors are chosen to exhibit low leakage current and low dielectric absorption.

The adjustable DC-voltage (V_{ref}) is buffered by an high-impedance chopper-stabilized OP-amplifier of unity gain and is then fed to the low-resistance leg of the stable voltage divider chain.

In designing this divider, contradictory demands arise. To reduce power consumption, the resistance should be as high as possible, but high-stability high-ohm resistors are difficult to manufacture and consequently very expensive. The solution was to make the divider from a number of moderate-precision resistors with the same nominal value, taken from the same factory batch to ensure equal temperature coefficient. The resistors forming R_1 are connected in series and those forming R_2 in parallel. The overall resistance in R_1 is chosen to draw 0.1 mA at maximum voltage. This typically results in

a reduction of the temperature coefficient with a factor of 20 for the division ratio compared to that of a single component. The only remaining problem is the unequal heating due to different currents in the series and parallel connected resistor elements and the resulting uneven power dissipation. In a test design of the 6kV-model this could be observed as a 2-minute time constant of about 50 ppm when changing from low to high output voltage. This was corrected by choosing 25 ppm/C instead of 50 ppm/C resistors and by lowering the value of the individual resistors to $1\text{M}\Omega$ from $2.2\text{M}\Omega$, consequently doubling the number of resistors building R_1 to 60. The voltage at the connection point between R_1 and R_2 is measured by a chopper-stabilized OP-amp. and then fed to the aforementioned capacitor and the coarse-regulated HV-generator.

The rectangle wave used to set the output voltage is defined from the computer and generated on a separate card, which is on ground potential. The duty cycle is variable in steps of 1 microsecond by means of a quartz-controlled counter. The used repetition rate is 250 Hz. This gives 4000 steps. The upper limit of the repetition rate is given by the desired precision in the output voltage. The lower limit is given by the desired voltage settling time due to longer RC time constants in the following low pass filter. The counter frequency is chosen to give sufficiently small steps to allow the use of standard $\pm 10\text{ V}$ DAC for fine adjustments. The important point is that the absolute value of a given step is considerably better than the step size as it is generated by the quartz-controlled counter. However, a constant voltage offset is added as a result of the rise-and falltimes in the counter logic and the previously mentioned analog switch. This voltage offset is measured at manufacture and compensated for by using a parameter table in the spectrometer control program. The linearity of the system up to the point V_{ref} is really better than 2 ppm, at least in short-term measurements.

The PWM signal is fed from the control card with its counters, to the supply card via a plastic optical fibre, by means of switching the light on and off according to the rectangle wave. This gives total galvanic separation between control system and voltage supplies.

3.4. Connection tree.

Spectra are collected in a constant dispersion mode, i.e. the voltage between the hemispheres is kept constant during a spectrum sweep. With the sample cell on ground potential, both hemispheres, as well as the edge and focusing electrodes have to follow the accelerating/retarding voltage AV. In our design, the supplies are connected in a "voltage tree", with all supplies which have to follow AV floating on that voltage. This design relaxes precision demands for most voltages and also enables fast sweeping of spectra. Only the AV-voltage and the less critical lens focusing voltage have to be swept during an experiment.

In experiments on photoelectrons or ions with low initial kinetic energies, the optimal kinetic energy in the analyzer is often inside the range of initial energies swept in the spectrum. Thus, it is necessary to be able to go continuously through zero with the AV voltage. Since the power supplies are built completely isolated from each other, this is easily achieved by connecting two power supplies with opposite polarities in series. The required total voltage is then converted to two suitable subvoltages of opposite polarities

using a simple algorithm in the computer program. The lens deflection voltage is supplied in the same fashion, in order to achieve zero-crossing capability.

As mentioned above, the step size and response time of the supplies are not adequate for the AV voltage. Therefore, the DAC module has to be incorporated. Sweeping is then performed by stepping the latter within a range of 22 V, and when this range is exceeded the main AV supply is changed by 22 V and the DAC is reset. For each of these major steps, the acquisition is halted for 1 sec. in order to let the voltages settle. Inside the 22 V range, spectra can be swept at maximum resolution at a rate which is limited only by the image frequency of the CCD camera, i.e. maximum 30 energy steps/sec.

The vacuum feedthroughs for the voltages are situated inside screen boxes, which also contain low pass filters and polarity switches, the latter to provide an economical way to enable fast conversion between energy analysis of electrons and positive ions. All interconnections of the supplies building the voltage tree are also made inside these boxes. The purpose of this is to exclude electromagnetic interference of both high and low frequencies from the electrode system. The screening is such that the noise and ripple levels inside the spectrometer are below 1 mV although the laboratory is situated on top of an electric motor installation creating 50 Hz fields strong enough to influence a TV monitor picture.

All power supplies are easily replaced, either for service or for change of range in order to achieve maximum precision in a given energy region.

3.5. The computer system.

The original control computer for the instrument was a Nuclear Data ND 6600 system. With its two LSI 11/2 processors, of which one was dedicated for handling the graphics, it was a quite advanced system for its time. Since the spectrometer program was written mainly in assembly-code and part of the data acquisition system was specially designed hardware it was, however, very difficult to modify for a changed spectrometer configuration or for changed types of experiments. With increasing age, service requirements became increasingly burdensome. The new control and data acquisition system for the spectrometer is based on a PC/AT-compatible computer and on the two dedicated 68000 microprocessors mentioned above, and the program is written entirely in Turbo Pascal. Identical programs and computer systems are used at four different electron spectrometers. We will here give a broad outline of the program and dwell on a few details of special interest for high-resolution work.

The main program for the spectrometer control contains routines for defining spectrum acquisition parameters, setting and stepping voltages, collecting and displaying data and saving them on disk, displaying earlier stored spectra, scaling and moving spectra and investigating the contents of individual channels. A set of auxiliary programs are used for such purposes as generation of correction tables for the detector energy scale, redefining such parameters as the calibration constants for the voltage supplies, measuring the same constants with an online precision voltmeter, and optimization of voltage settings with respect to resolution and intensity. Since the computer is of a single-task type, spectral data are transferred to a larger computer for further analysis, and consequently no data analysis is included in the spectrometer program.

All communication between the AT and the peripheral units (voltage supplies and detector interface) takes place via an IEEE-488 standard port and is in ASCII-format. Likewise,

spectral data are stored as text files in a format compatible with the CRUNCH analysis package ¹⁵ Complementary data for each spectrum are stored on separate text files.

The parameters necessary to define voltage settings, translation between CCD camera line number and energy, collection times etc. are of different degree of permanence. Thus, e.g. start and stop energies, energy step sizes, pass energy and collection times are in principle individual for each spectrum, while e.g. the sphere voltages corresponding to a certain analyzer pass energy or the parameters defining the CCD properties would hardly ever be changed. This is reflected in the program structure, insofar that the most permanent parameters are stored in tables which can only be changed outside the main program, while parameters characteristic for each spectrum are defined by editing the template for each spectral region.

Our standard method of collecting spectra consists in sweeping the spectral region of interest over the multidetector by stepping the AV voltage. This sweeping technique serves two purposes, namely to allow arbitrarily long spectra to be recorded independent of the width of the multidetector and to average out variations in the detector sensitivity function. Although this technique has been used for a long time in our laboratory and has been described earlier ¹⁶, it seems not to be well-known and we therefore give a short description here. The registered pulses from the MCP initially are sorted in a number of physical channels, in our case corresponding to the lines of the CCD array. The information contained in these physical channels then has to be transformed to count rates in a number of logical channels corresponding to equidistant energy steps in the spectrum. The energy difference of any physical channel from some reference point (e.g. the centre of the detector) is stored in a look-up table which is generated by a calibration procedure described below and available in the interface microprocessor. The actual energy corresponding to a certain physical channel is obtained as the sum of this energy difference and the energy offset of the reference point corresponding to the actual value of the AV voltage. The counts from each physical channel are then added to the logical channel closest to that energy. As the AV voltage is stepped, the logical channels scan over the array of physical channels. Although in general the number of physical channels is not an integer multiple of the number of simultaneously active logical channels, this stepping procedure ensures that all logical channels get the same contribution from any given physical channel during every sweep.

During the scanning of a logical channel over the physical channel array the partial sums are stored in an intermediate buffer in the interface, and only when it has completed this scan is the final sum transferred to the main computer, thus minimizing the amount of data transfer.

Definition of an experiment thus consists in setting up the parameters defining a number of regions, each of which can have individually chosen energy range and step size, acquisition time, pass energy, and detector window. The total acquisition time for a region can be chosen both by choosing the time per energy steps (in units of camera frames) and the number of sweeps over the region. An experiment (a run) may consist of up to 20 different energy regions. Concerning the sweeping strategy, one can distinguish two different cases, since both energies and intensities can exhibit slow drifts during the acquisition of a spectrum. In one extreme case, the primary interest is in obtaining maximum resolution of adjacent structures, while energy differences or intensity ratios over larger energy ranges are of secondary interest. In this case, it is advantageous to scan the spectrum just once, with a sweep rate chosen to give adequate statistics. In the opposite extreme case, one instead makes a fairly large number (several hundreds) of

rapid sweeps over the spectrum. This averages out intensity variations and eliminates the risk of systematic energy shifts between different parts of the spectrum. On the other hand, one in this case often observes that slow energy drifts smear out fine structure in the spectrum. In order to at least partly remedy this, we have introduced a calculation of the correlation function between data acquired during one sweep and the sum of all previous sweeps. The data from the last sweep are then shifted by an amount corresponding to the maximum in the correlation function before adding. This requires that there is enough statistically significant structure in each sweep to allow a reliable calculation of the correlation function. If this is not the case for the region of interest, it is possible to define an extra energy region containing strong and narrow structures in order to determine the shift, and running these regions alternately.

While the setting up of experiments is done via editing of a template, manipulation of the graphical display of spectra is controlled via the computer's function keys. Spectra can be rescaled for inspection during an experiment, although this interrupts the collection of data for a short period.

As mentioned, the tables defining the correspondence between energy offset and the CCD line number have to be generated experimentally. There is one such table for each of the values of analyzer pass energy used, since e.g. work function modifications of electrode potentials do not scale with the applied voltages. Major adjustments of the edge or focusing voltages may necessitate adjustment of these tables, and consequently a reasonably fast procedure for this has to be available. In our present set-up, this calibration is performed by recording a narrow line using a succession of 10-20 narrow windows (i.e. just a few CCD-lines) at different positions of the detector. The apparent energy positions of the peak in the different windows are then used in a separate program to generate a correction to the previously used table. The energy position for each camera line is calculated using a cubic spline interpolation through the 10-20 measured points.

For optimizing the spectrometer performance (resolution and intensity) a separate program is used, where all voltages can be set and stepped individually or in groups using simple "arrow up/down" keys on the computer. Line shapes can be observed in real time on the TV-monitor or collected for more quantitative evaluation of width, shape and intensity.

4. ACKNOWLEDGEMENT:

The computer program for spectrometer control was developed by Ing. Hans Rydåker.

5. REFERENCES.

1. H. Siegbahn and L. Karlsson, Handbuch der Physik, Vol. 31 (ed. W. Mehlhorn), Springer Verlag, 1982.
2. R.C.G. Leckey, J. Electron Spectrosc. Relat. Phenom. 43, 183 (1987).
3. B. Wannberg, H. Veenhuizen, L. Mattsson, K.-E. Norell and K. Siegbahn, Uppsala University Institute of Physics Report, UIIP-1108, 1984.
4. A.H. Snell, ed. Nuclear Instruments and their uses, p.218. Wiley, New York 1962.
5. S. Svensson, L. Karlsson, P. Baltzer, B. Wannberg, U. Gelius and M. Y. Adam, J. Chem. Phys. 89, 7193 (1988).
6. L. Karlsson, P. Baltzer, S. Svensson and B. Wannberg, Phys. Rev. Lett. 60, 2473 (1988).
7. S. Svensson, L. Karlsson, P. Baltzer, M.P. Keane and B. Wannberg, Phys. Rev. A40, 4369 (1989).
8. B. Wannberg, S. Svensson, M.P. Keane, L. Karlsson and P. Baltzer, Chem. Phys. 133, 281 (1989).
9. P.G. Fournier, G. Comtet, J. Fournier, P. Millie, J.H.D. Eland, S. Price, S. Svensson, P. Baltzer, B. Wannberg, L. Karlsson and U. Gelius, J. Chem. Phys. 89, 3553 (1988).
10. A. Cesar, H. Ågren, A. Naves de Brito, S. Svensson, L. Karlsson, M.P. Keane, B. Wannberg, P. Baltzer, P.G. Fournier and J. Fournier, J. Chem. Phys. 93, 918 (1990).
11. P. Baltzer, B. Wannberg, S. Svensson and L. Karlsson. Uppsala University Institute of Physics Report, UIIP-1190, 1988.
12. P. Baltzer, L. Karlsson, S. Svensson, and B. Wannberg, J. Phys. B: At. Mol. Opt. Phys 23, 1537 (1990).
13. H. Wollnik, T. Matsuo and H. Matsuda, Nucl. Instr. and Meth. 102, 13 (1972).
14. H. Wollnik, Nucl. Instr. and Meth. 52, 250 (1967).
15. R.P. Vasques, J.D. Klein, J.J. Barton and F.J. Grunthaner, J. Electron Spectrosc. Relat. Phenom. 23, 63 (1981).
16. E. Basilier, Uppsala University Institute of Physics Report, UIIP-1022, 1980.

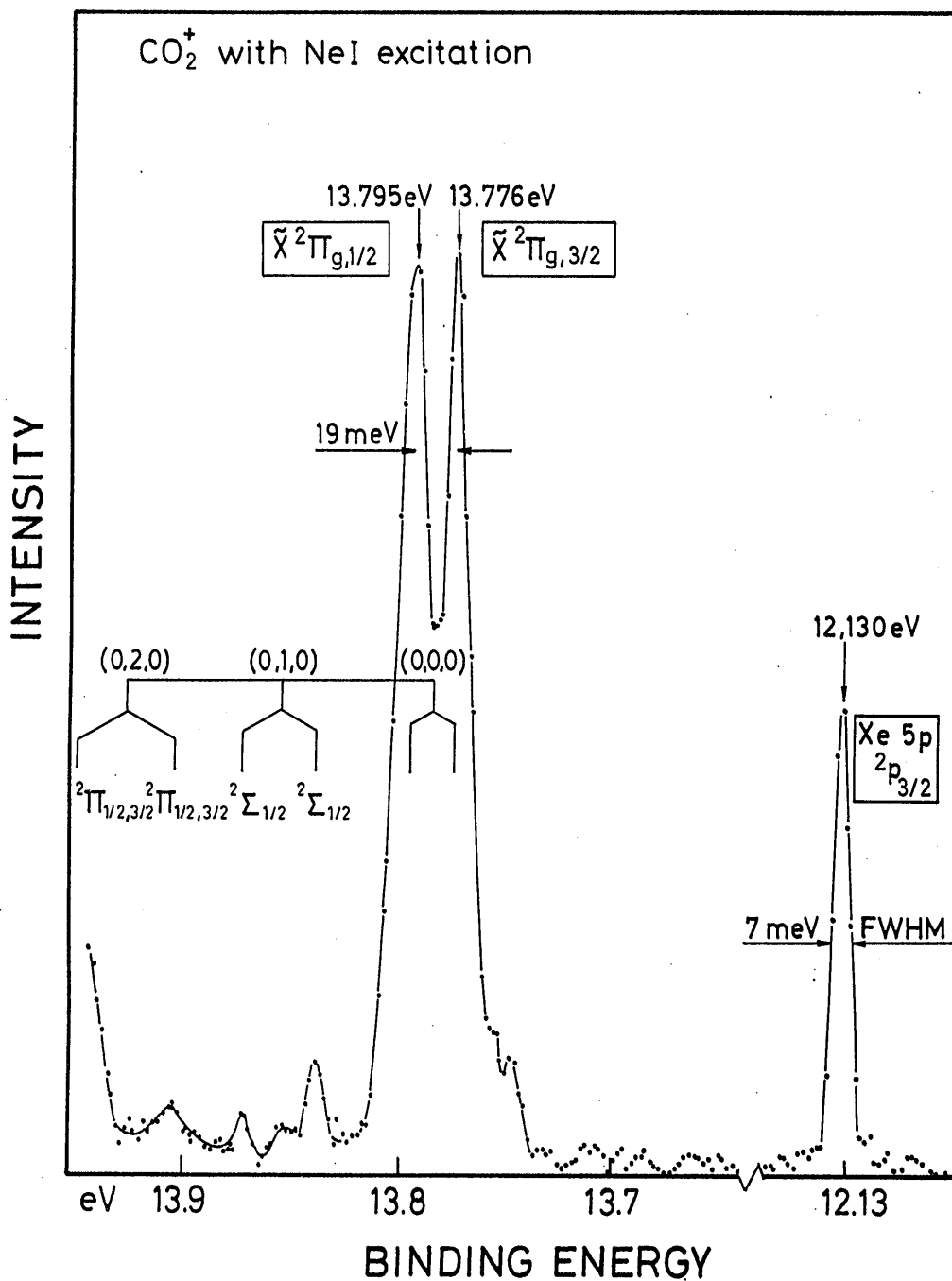


Fig 1. Photoelectron spectra from Xe and CO_2 obtained with the present instrument. The bar diagram shows Renner-Teller components in the bending vibrational mode ν_2 .

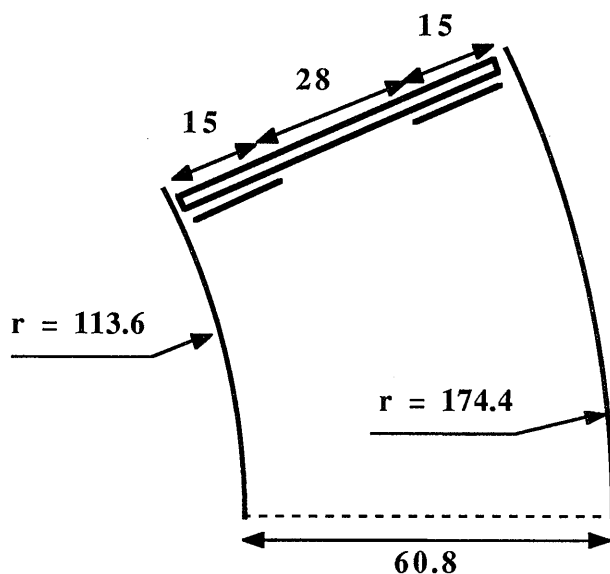


Fig. 2. Cross section of the analyzer with its fringing field electrodes. The widths of the terminating electrodes are chosen such that agreement with a perfect spherical field up to third order can be achieved with the backing electrode on the AV potential.

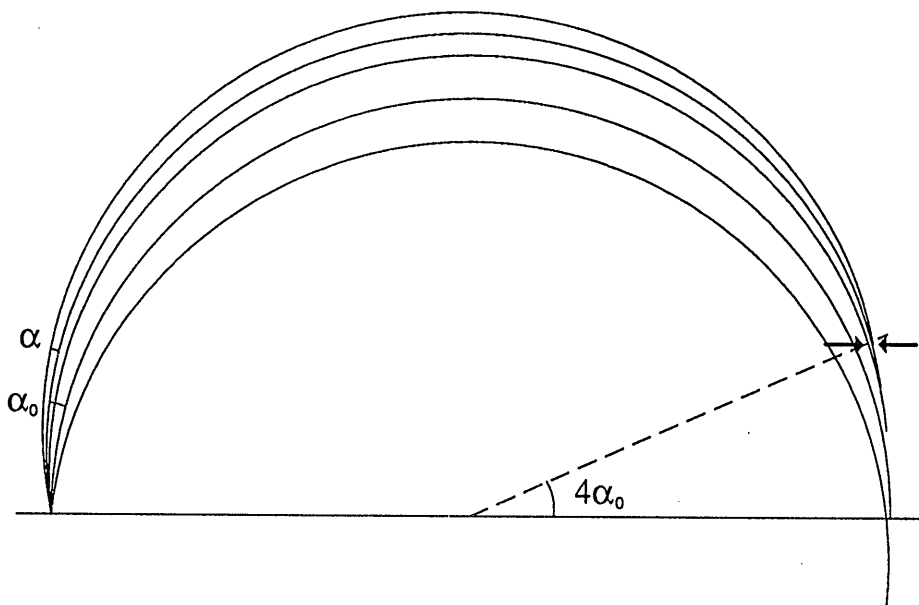


Fig. 3. A pencil of trajectories centered around an entrance direction with an angle α_0 against the central equipotential surface in an hemispherical analyzer is focused after an angle which differs by $4\alpha_0$ from 180° .

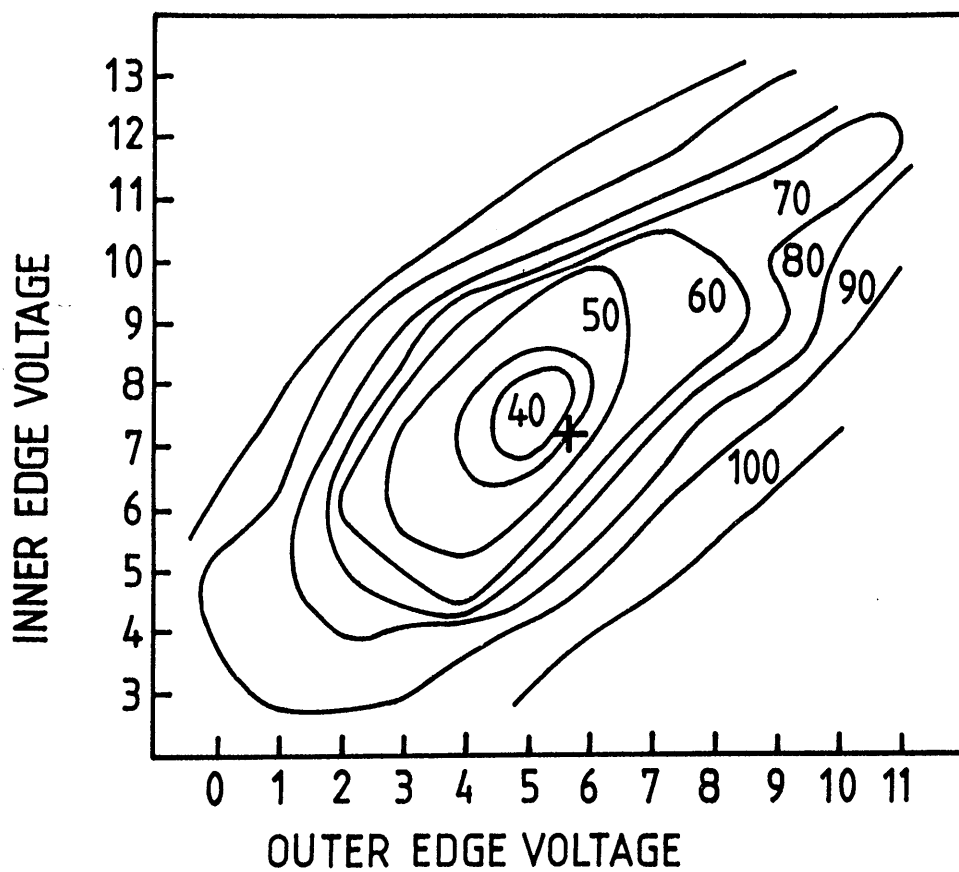


Fig. 4. The width (FWHM) of a photoelectron line (averaged over width of multidetector) for different combinations of the edge plate voltages in the analyzer. The analyzer pass energy is 20 eV. The condition giving the best approximation to a spherical field is marked by a cross.

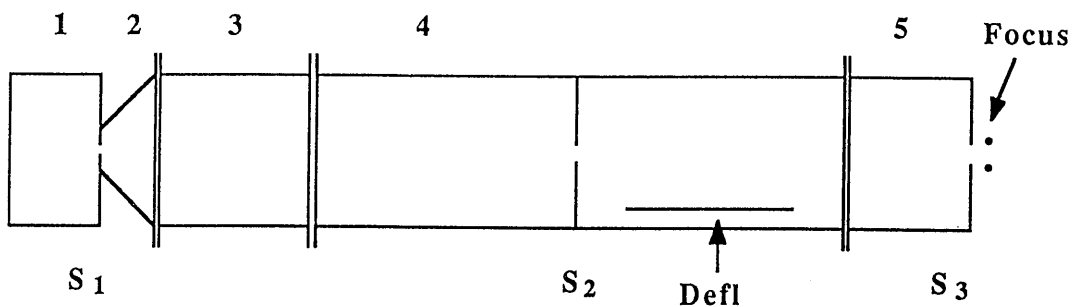


Fig. 5. Schematic cross section of the lens system and the gas cell. The deflection electrode is a semicylinder, centered on the lens axis.

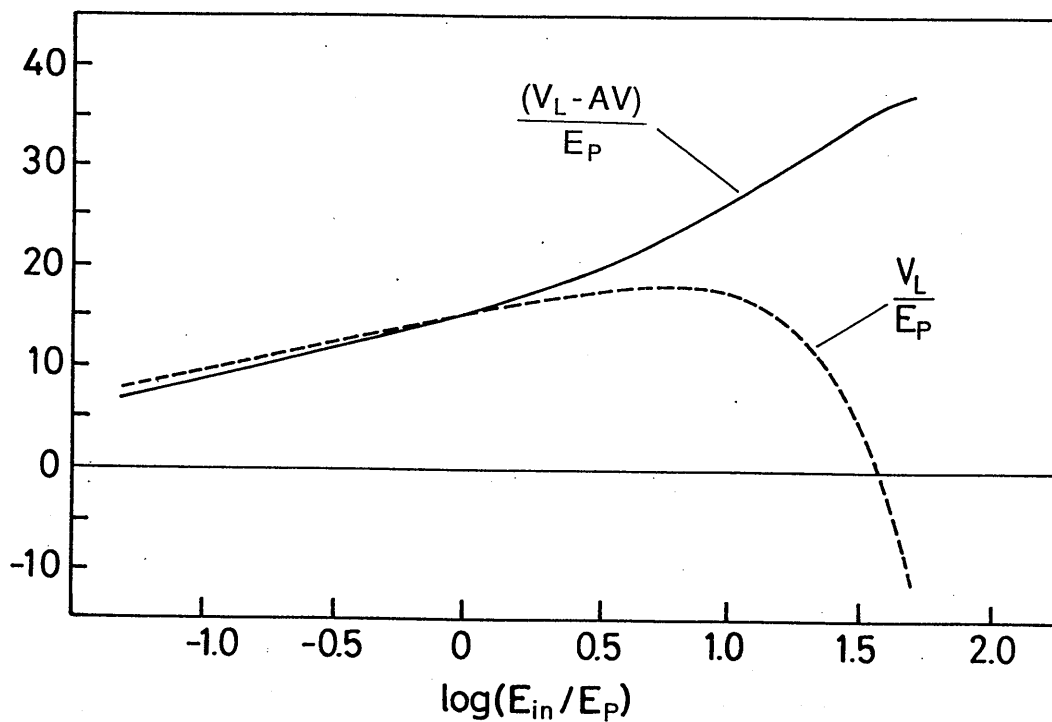


Fig. 6. The universal curve for the focusing voltage in the lens. Focusing voltage and initial energy are both given in units of the pass energy in the analyzer.

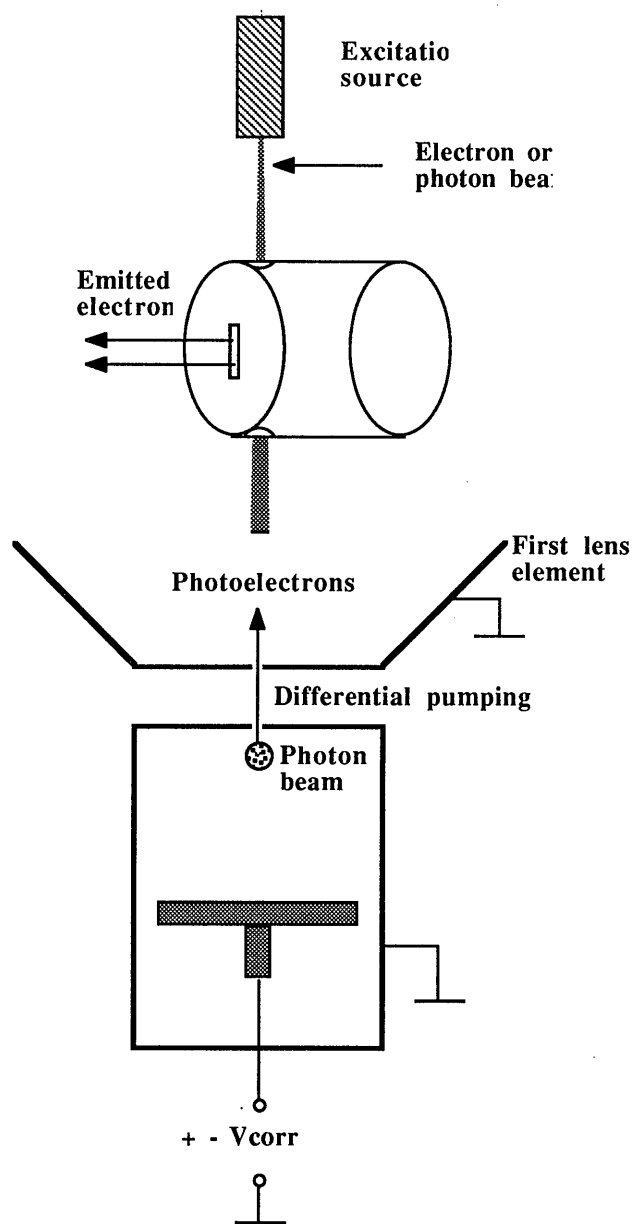


Fig. 7. Schematic drawing of the gas cell (top) and a schematic cross section of it with the compensating electrode (bottom).

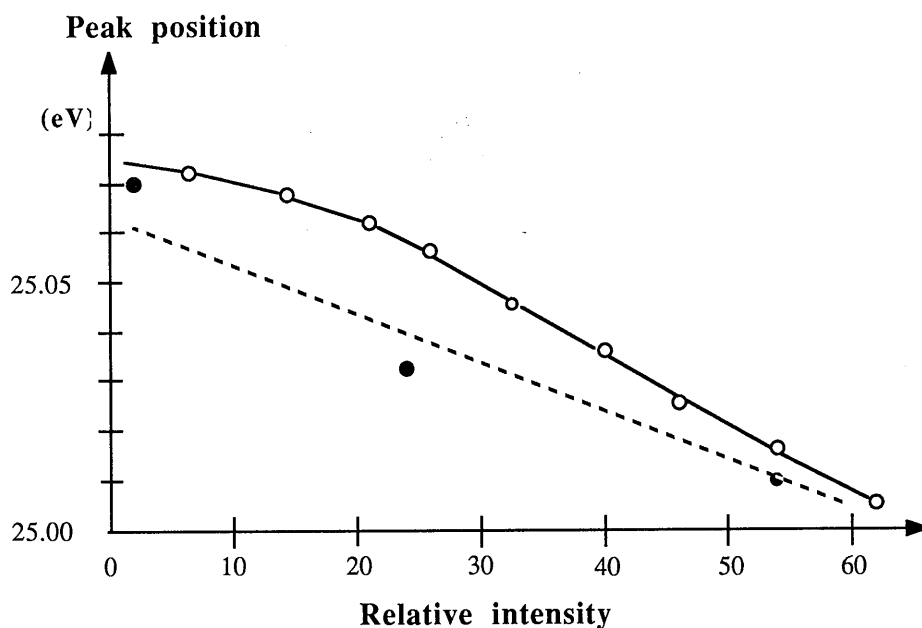


Fig. 8. The interdependence between intensity and energy shift for the Ar 3p photoelectron lines excited by HeII α radiation (40.8 eV). Open circles denote results with maximum light intensity and different Ar pressures in the gas cell. Filled circles denotes results at the highest pressure but with reduced light intensity. Results indicate that the total ion density in the excitation region play an important part in line shifts and broadenings. It should be noted that the radiation was unfiltered and consequently the ionization was primarily from 21.22 eV HeI resonance light.

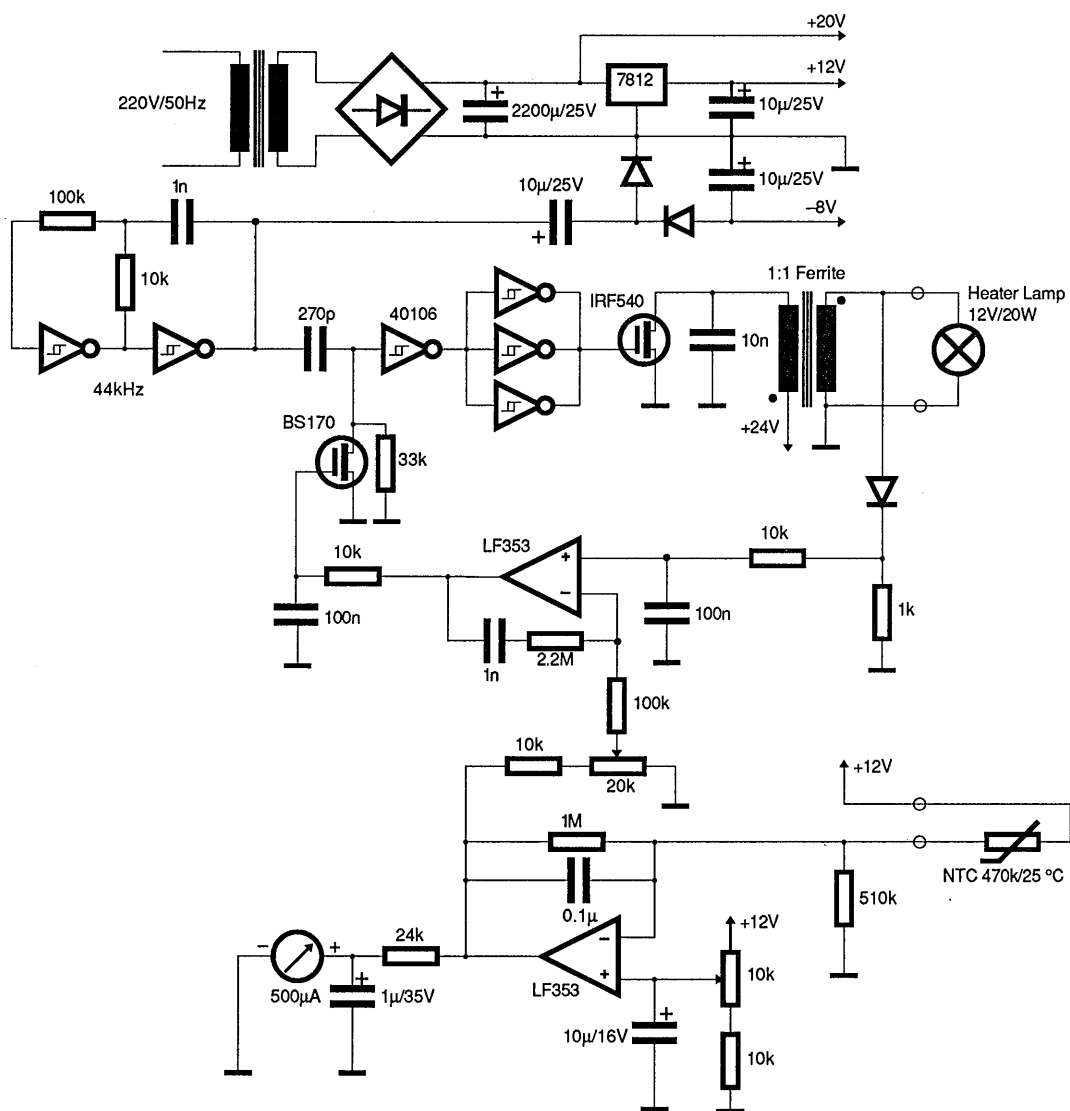


Fig 9. The controller electronics for the gas cell oven.

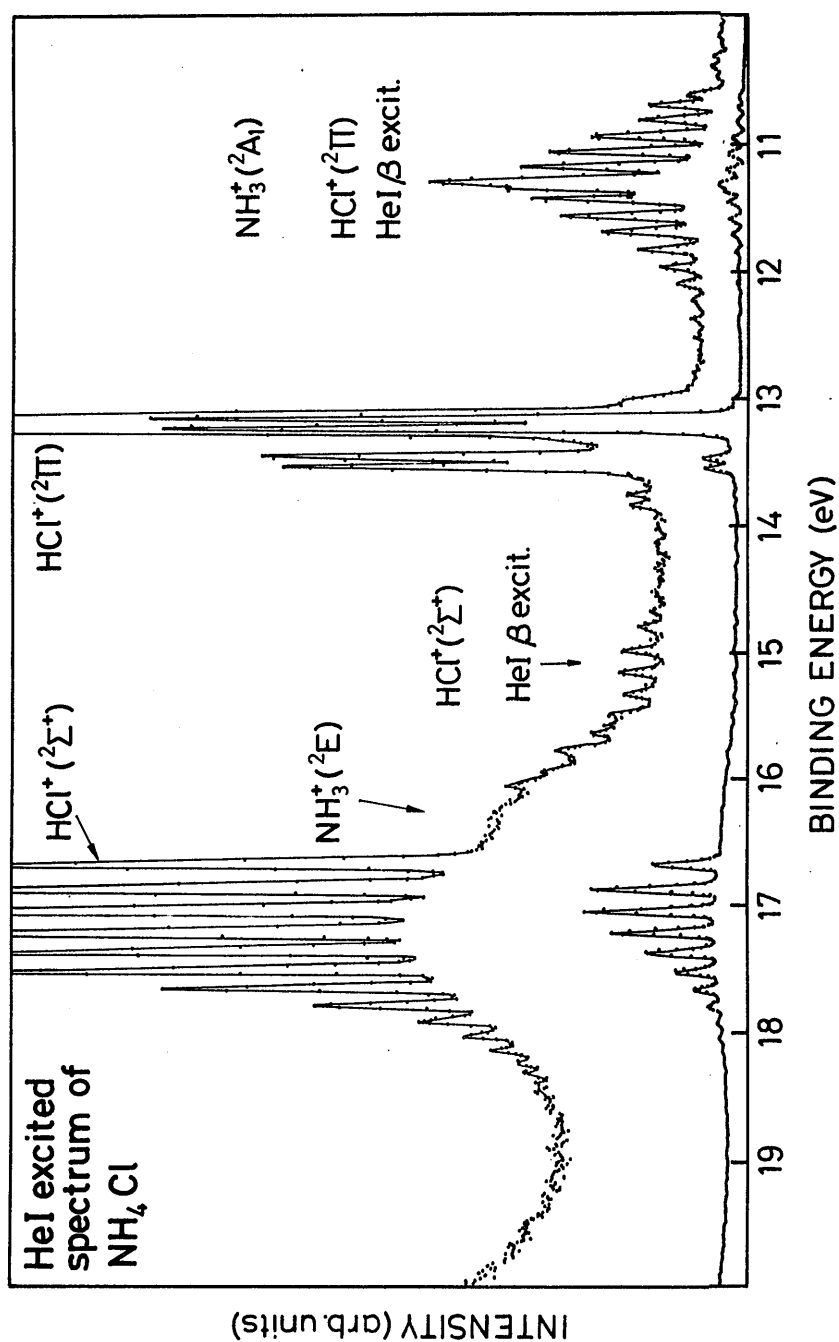


Fig. 10. Photoelectron spectra from ammonium chloride recorded with the gas cell heated to approx. 150C° . The substance is decomposing into HCl and NH_3 . No degradation of the spectrometer resolution can be seen.

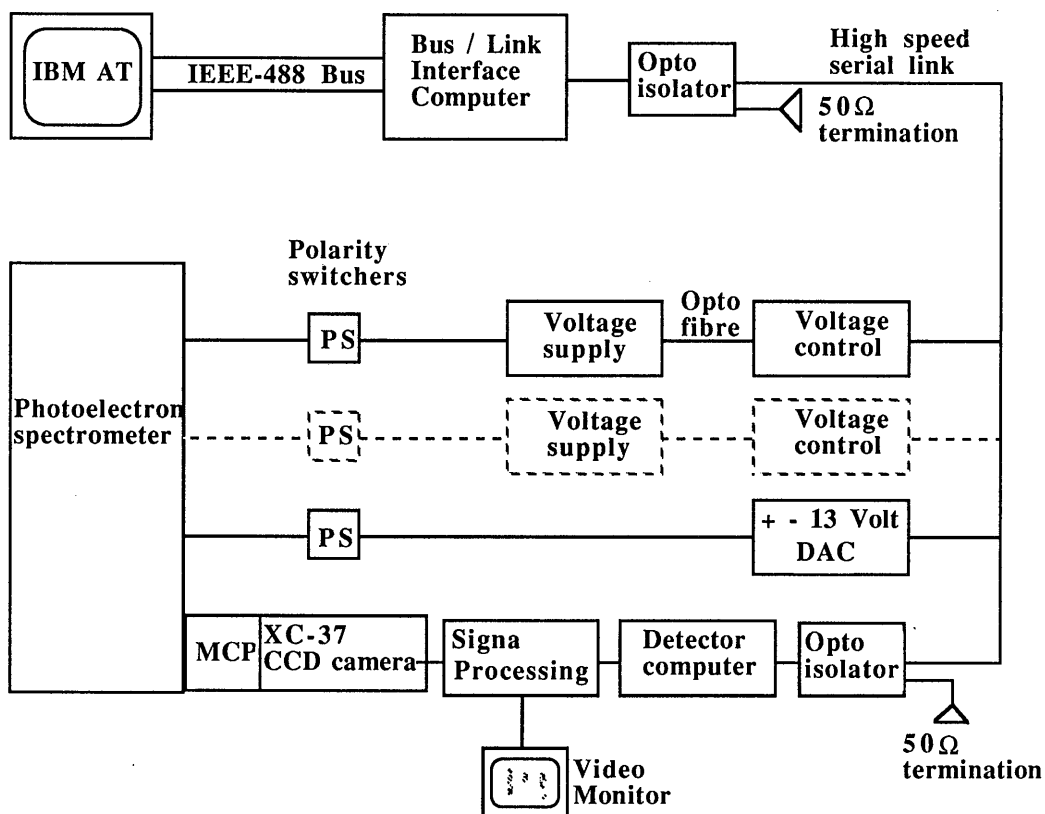


Fig. 11. General scheme of the spectrometer control system.

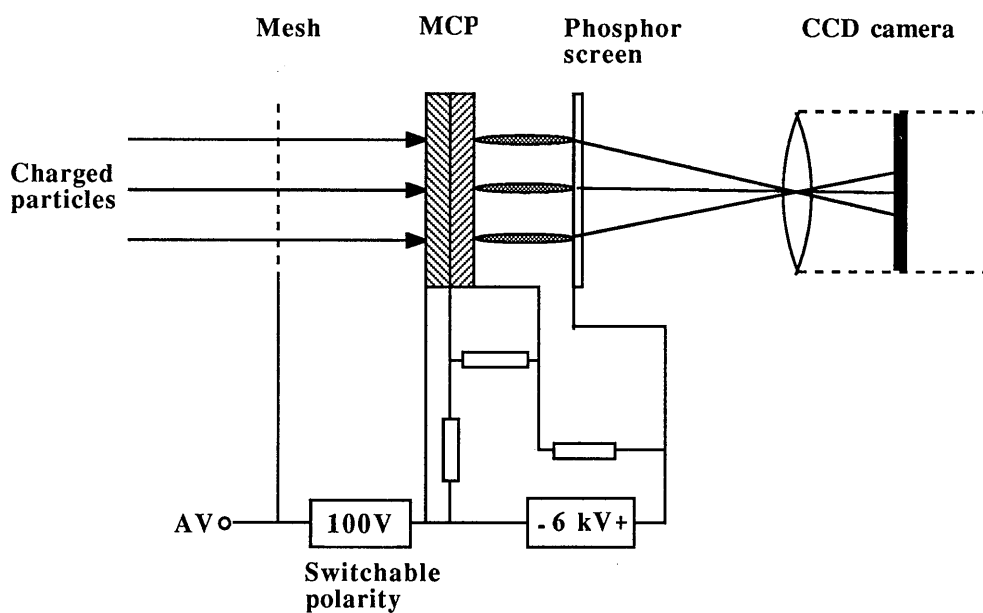


Fig. 12. Schematic drawing of the detection system.

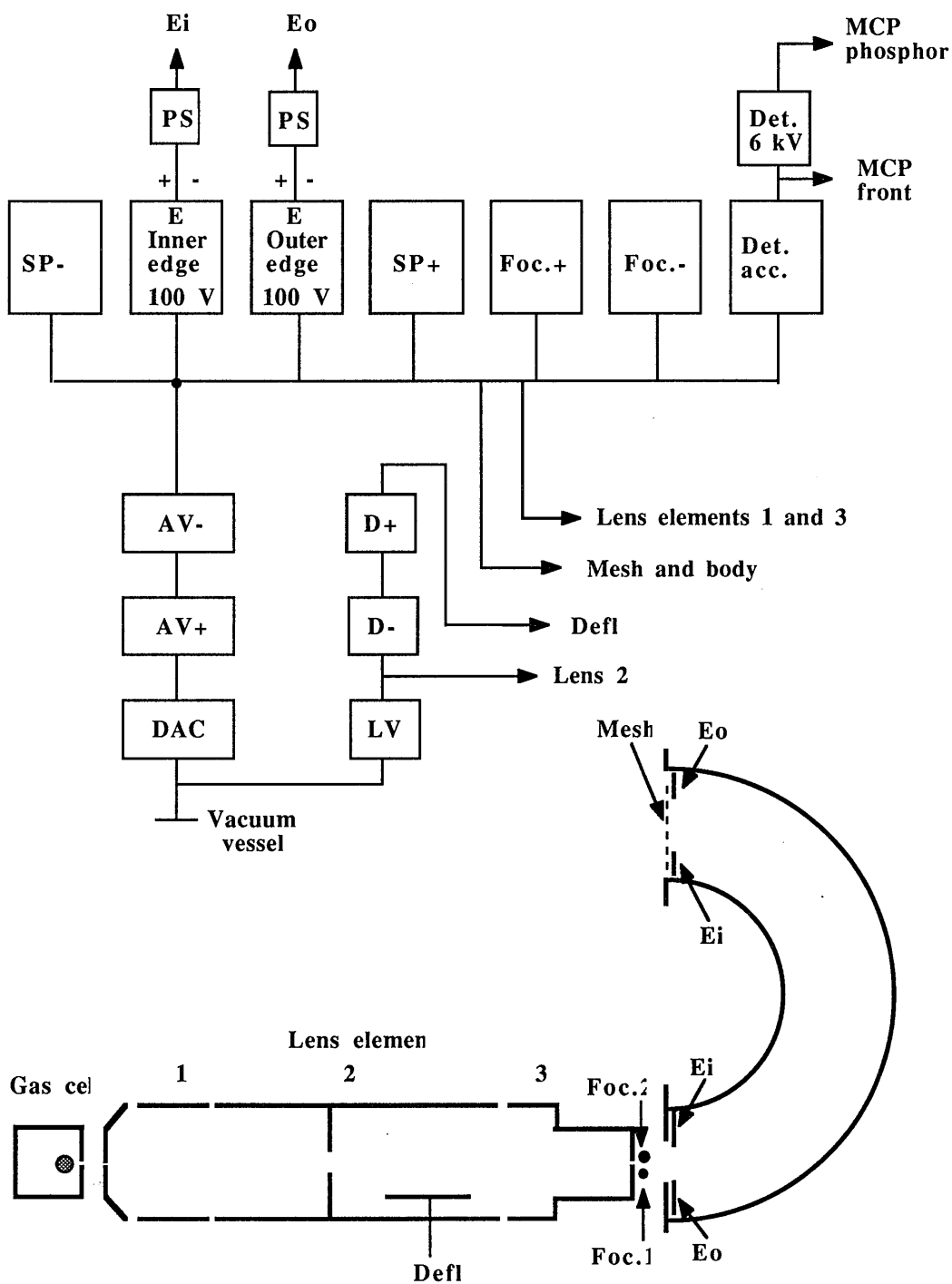


Fig. 13. Schematic drawing of the interconnections of the 14 voltage supplies for the spectrometer. Each voltage supply is totally isolated from earth. A drawing of the spectrometer electrodes is shown below.

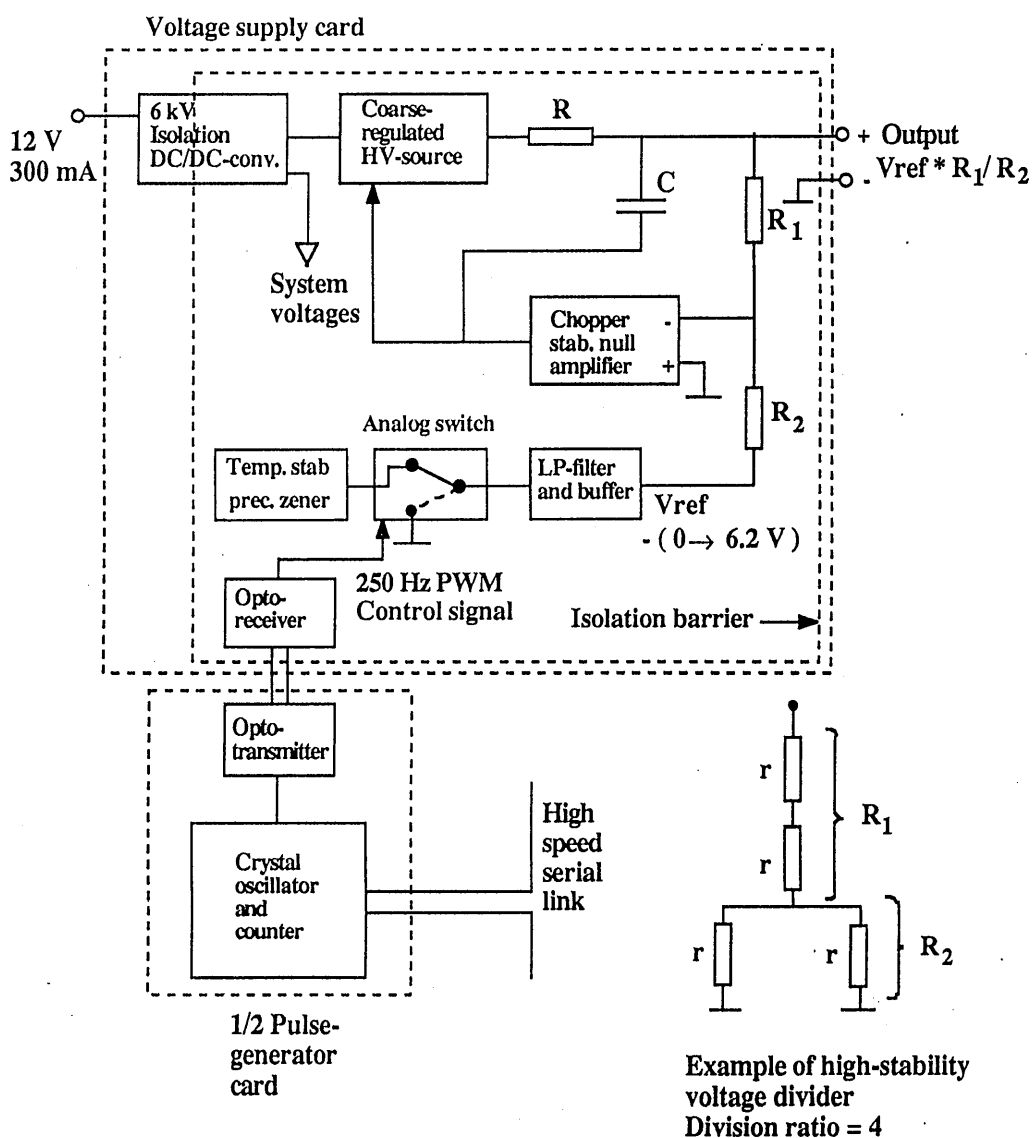


Fig. 14. Functional blocks of the highly stable voltage supply.